

Title	Pattern formation in a two-layered Benard convection (Mathematical Analysis in Fluid and Gas Dynamics)
Author(s)	Fujimura, Kaoru
Citation	数理解析研究所講究録 (2002), 1247: 79-96
Issue Date	2002-01
URL	http://hdl.handle.net/2433/41738
Right	
Type	Departmental Bulletin Paper
Textversion	publisher

Pattern formation in a two-layered Bénard convection

鳥取大・工 藤村 薫 (Kaoru Fujimura)

*Department of Applied Mathematics and Physics
Tottori University, Tottori 680-8552, Japan*

The resonant interaction between steady modes with wavenumbers in the ratio 2:1 has been examined for its pattern formation on a hexagonal lattice. Twelve-dimensional amplitude equations of the cubic order are derived by means of the center manifold reduction. With the aid of the equivariant bifurcation theory, steady solutions of the equations due to the primary and the secondary bifurcations are classified and the orbital stability of them are analyzed. The analyses are extended to two-layered Rayleigh-Bénard convection with a non-deformable thin interface, which provides the exact resonance between the critical modes as had been found by Proctor and Jones [10]. In order for the cubic amplitude equations to be generic, the self-adjointness of the operators in the linearized problem needs to be broken. For this purpose, we took account of the quadratic density profile as a function of the temperature. All the primary and the secondary steady patterns obtained are found to be unstable except for the super hexagonal pattern which is composed of hexagonal pattern and double sized one.

1. Introduction

In the presence of $O(2)$ -symmetry, the resonant interaction between steady modes with wavenumbers in the ratio 2:1 is governed by

$$\dot{z}_1 = f_1(z_1, z_2, \mu), \quad \dot{z}_2 = f_2(z_1, z_2, \mu), \quad z_1, z_2 \in \mathbf{C}, \quad \mu \in \mathbf{R}^2, \quad (1)$$

where the vector field is expressed in terms of $O(2)$ -equivariant polynomials and invariant functions such that

$$\begin{aligned} f_1(z_1, z_2, \mu) &= z_1 p_1(u, v, w, \mu) + \bar{z}_1 z_2 q_1(u, v, w, \mu), \\ f_2(z_1, z_2, \mu) &= z_2 p_2(u, v, w, \mu) + z_1^2 q_2(u, v, w, \mu). \end{aligned} \quad (2)$$

Here, $u = |z_1|^2$, $v = |z_2|^2$, and $w = \bar{z}_1^2 z_2 + z_1^2 \bar{z}_2$ are $O(2)$ -invariants, z_1 , z_2 , $\bar{z}_1 z_2$, and z_1^2 are generators of the $O(2)$ -equivariant vector field, and p_1 , p_2 , q_1 , and q_2 are real valued invariant functions of u , v , and w . See Buzano and Russo [3] for further details.

Taylor expanding p_1 , p_2 , q_1 , and q_2 about the origin and truncating the resultant equations at the cubic order, we obtain

$$\begin{aligned} \dot{z}_1 &= \sigma_1 z_1 + \beta_1 \bar{z}_1 z_2 + \lambda_{11} |z_1|^2 z_1 + \lambda_{21} |z_2|^2 z_1, \\ \dot{z}_2 &= \sigma_2 z_2 + \beta_2 z_1^2 + \lambda_{12} |z_1|^2 z_2 + \lambda_{22} |z_2|^2 z_2. \end{aligned} \quad (3)$$

Analyses on the steady state solutions of (3) have been done, eg., by Dangelmayr[5], in detail. Equations (3) have three non-trivial steady state solutions as fixed points. They are steady state S_2 given by $u = 0$ and $v = 0$, and asymmetric steady states S_{\pm} given by $u, v > 0$, $z_2 \in \mathbf{R}$, and $\cos[2 \arg(z_1) - \arg(z_2)] = \pm 1$. As relative equilibria, a traveling wave bifurcates from S_{\pm} . It has the property that $u, v > 0$, $\frac{d}{dt}[2 \arg(z_1) - \arg(z_2)] = 0$, and $\cos[2 \arg(z_1) - \arg(z_2)] = \pm 1$. Standing waves bifurcate from the asymmetric steady states whereas modulated waves bifurcate from the traveling wave due to Hopf bifurcation. Proctor and Jones [10] and Armbruster,

Guckenheimer and Holmes [1] clarified the existence of structurally stable heteroclinic cycles. Very recently, new heteroclinic cycles far from the mode interaction point were extensively investigated by Porter and Knobloch[9]. So far, all the results above exhibit one-dimensional variation in the planform: the spatial pattern caused by the resonance varies periodically in one horizontal direction. A question naturally arises whether the solutions mentioned above are stable in the framework of two-dimensional pattern formation problem. Standard way to answer the question is to examine the resonance on a square or a hexagonal lattice. We focus ourselves on the pattern formation on the latter lattice.

2. Eigenfunction expansion and center manifold reduction

In this section, we formally derive the amplitude equations governing the weakly nonlinear evolution of exactly resonating modes on a hexagonal lattice. We assume our physical system has an infinite extent in the horizontal xy -plane. Consider a situation where three-dimensional disturbance $\psi(x, y, z, t)$ is added to the basic field which is homogeneous and isotropic in the horizontal plane. Here, the vector ψ may be composed of velocity, temperature, magnetic field, etc. Let us start with the nonlinear PDE governing $\psi(x, y, z, t)$ having the form

$$\frac{\partial}{\partial t} S\psi = \mathcal{L}(\mu)\psi + \mathcal{N}(\psi, \psi), \quad (4)$$

where S and \mathcal{L} denote linear operators involving spatial derivatives, \mathcal{N} denotes quadratic nonlinear terms, and $\mu \in \mathbf{R}^2$ denote control parameters. These S , \mathcal{L} , and \mathcal{N} are assumed to have no explicit dependence on either x , y , or t . Explicit form of S , \mathcal{L} , and \mathcal{N} will be given in §4 for two-layered Rayleigh-Bénard convection.

2.1. Expansions in Fourier series and linear eigenfunctions

The linearized equations of (4) subject to appropriate boundary conditions provide a linear eigenvalue problem. We assume the eigenvalues discrete and simple. Denote the j -th eigenvalue by $\sigma^{(j)}$ and the eigenfunction belonging to $\sigma^{(j)}$ by $\psi^{(j)}$. The eigenvalue problem is given by

$$\mathcal{L}(\mu)\psi^{(j)}(x, y, z) = \sigma^{(j)} S\psi^{(j)}(x, y, z), \quad j \geq 1, \quad (5)$$

with appropriate boundary conditions for $\psi^{(j)}$. Let the eigenvalues $\sigma^{(j)}$ be ordered in a descending manner such that

$$\operatorname{Re} \sigma^{(1)} > \operatorname{Re} \sigma^{(2)} > \operatorname{Re} \sigma^{(3)} > \dots$$

We assume that $\operatorname{Re} \sigma^{(1)} = 0$ and $\operatorname{Re} \sigma^{(j)} < 0$ for $j \geq 2$. The corresponding eigenfunction $\psi^{(1)}(x, y, z)$ belonging to $\sigma^{(1)}$ is assumed to be a linear combination of twelve exponential factors

$$\begin{aligned} & e^{\pm ik_c x}, \quad e^{\pm ik_c (-\frac{1}{2}x + \frac{\sqrt{3}}{2}y)}, \quad e^{\pm ik_c (-\frac{1}{2}x - \frac{\sqrt{3}}{2}y)}, \\ & e^{\pm 2ik_c x}, \quad e^{\pm 2ik_c (-\frac{1}{2}x + \frac{\sqrt{3}}{2}y)}, \quad e^{\pm 2ik_c (-\frac{1}{2}x - \frac{\sqrt{3}}{2}y)}. \end{aligned} \quad (6)$$

We set

$$E_1 = e^{ik_c x}, \quad E_2 = e^{ik_c (-\frac{1}{2}x + \frac{\sqrt{3}}{2}y)}. \quad (7)$$

All the factors in (6) are expressed in terms of E_1 and E_2 as $E_1^m E_2^n$ for $m, n \in \mathbf{Z}$. Especially, $e^{\pm ik_c (-\frac{1}{2}x - \frac{\sqrt{3}}{2}y)} = E_1^{\mp 1} E_2^{\mp 1}$.

We Fourier decompose $\psi^{(j)}(x, y, z)$ as

$$\psi^{(j)} = \sum_{m,n} \phi_{mn}^{(j)}(z) E_1^m E_2^n. \quad (8)$$

The Fourier coefficient $\phi_{mn}^{(j)}(z)$ satisfies the linear eigenvalue problem

$$L_{mn}(\mu)\phi_{mn}^{(j)} = \sigma_{mn}^{(j)} S_{mn} \phi_{mn}^{(j)}, \quad (9)$$

subject to appropriate boundary conditions for $\phi_{mn}^{(j)}$ where

$$L_{mn} = \mathcal{L}|_{\partial_x \rightarrow i(m-\frac{n}{2})k_c, \partial_y \rightarrow i\frac{\sqrt{3}}{2}nk_c, \partial_z \rightarrow d/dz},$$

$$S_{mn} = \mathcal{S}|_{\partial_x \rightarrow i(m-\frac{n}{2})k_c, \partial_y \rightarrow i\frac{\sqrt{3}}{2}nk_c, \partial_z \rightarrow d/dz}.$$

The adjoint problem corresponding to (9) is defined by

$$\tilde{L}_{mn}(\mu)\tilde{\phi}_{mn}^{(j)} = \sigma_{mn}^{(j)} \tilde{S}_{mn} \tilde{\phi}_{mn}^{(j)}, \quad (10)$$

with

$$\langle \tilde{\phi}_{mn}^{(j)}, (L_{mn}(\mu) - \sigma_{mn}^{(j)} S_{mn}) \phi_{mn}^{(j)} \rangle = \langle (\tilde{L}_{mn}(\mu) - \sigma_{mn}^{(j)} \tilde{S}_{mn}) \tilde{\phi}_{mn}^{(j)}, \phi_{mn}^{(j)} \rangle,$$

where $\langle \cdot, \cdot \rangle$ denotes an appropriate inner product.

We assume that all the linear eigenvalues $\sigma_{mn}^{(j)}$ are simple and the eigenfunctions $\phi_{mn}^{(j)}$ belonging to $\sigma_{mn}^{(j)}$ are orthogonal and complete. Let us now expand $\psi(x, y, z, t)$ in Fourier series and linear eigenfunctions:

$$\psi(x, y, z, t) = \sum_{m=-\infty}^{\infty} \sum_{n=-\infty}^{\infty} \sum_{j=1}^{\infty} A_{mn}^{(j)}(t) \phi_{mn}^{(j)}(z) E_1^m E_2^n. \quad (11)$$

The reality condition gives $A_{-m-n}^{(j)} = \bar{A}_{mn}^{(j)}$ where an overbar denotes the complex conjugate. Substituting (11) into (4) and taking the inner products with the adjoint functions $\tilde{\phi}_{mn}^{(j)}$, we obtain amplitude equations for $A_{mn}^{(j)}$:

$$\dot{A}_{mn}^{(j)} = \sigma_{mn}^{(j)}(\mu) A_{mn}^{(j)} + \sum_{k,l} \lambda_{k,l,m-k,n-l}^{(j,p,q)} A_{k,l}^{(p)} A_{m-k,n-l}^{(q)}, \quad (12)$$

where

$$\sigma_{mn}^{(j)}(\mu) = \frac{\langle \tilde{\phi}_{mn}^{(j)}, L_{mn}(\mu) \phi_{mn}^{(j)} \rangle}{\langle \tilde{\phi}_{mn}^{(j)}, S_{mn} \phi_{mn}^{(j)} \rangle}, \quad \lambda_{k,l,m-k,n-l}^{(j,p,q)} = \frac{\langle \tilde{\phi}_{mn}^{(j)}, N(\phi_{kl}^{(p)}, \phi_{m-k,n-l}^{(q)}) \rangle}{\langle \tilde{\phi}_{mn}^{(j)}, S_{mn} \phi_{mn}^{(j)} \rangle}.$$

2.2. Center manifold reduction

The center manifold theorem guarantees that the amplitude of stable modes $A_{mn}^{(j)}$ with $(m, n, j) = (\pm 1, 0, 1), (0, \pm 1, 1), (\mp 1, \mp 1, 1), (\pm 2, 0, 1), (0, \pm 2, 1), (\mp 2, \mp 2, 1)$ is expressed by

$$A_{mn}^{(j)} = h_{mn}^{(j)}(A_{\pm 10}^{(1)}, A_{0\pm 1}^{(1)}, A_{\mp 1\mp 1}^{(1)}, A_{\pm 20}^{(1)}, A_{0\pm 2}^{(1)}, A_{\mp 2\mp 2}^{(1)}). \quad (13)$$

See [4]. The function $h_{mn}^{(j)}$ satisfies $h_{mn}^{(j)}(0) = dh_{mn}^{(j)}(0) = 0$ where $dh_{mn}^{(j)}$ is the Jacobian derivative of $h_{mn}^{(j)}$. We may expand $h_{mn}^{(j)}$ in terms of $A_{\pm 10}^{(1)}, A_{0\pm 1}^{(1)}, A_{\mp 1\mp 1}^{(1)}, A_{\pm 20}^{(1)}, A_{0\pm 2}^{(1)}$, and $A_{\mp 2\mp 2}^{(1)}$ and truncate

(13) at the quadratic order in order to derive the cubic amplitude equations. Therefore $h_{mn}^{(j)}$ is expressed as

$$h_{mn}^{(j)} = \sum_{k_1, k_2, l_1, l_2} \gamma_{k_1 k_2 l_1 l_2}^{(j)} A_{k_1 k_2}^{(1)} A_{l_1 l_2}^{(1)} + O(3). \quad (14)$$

Substituting (14) into (12) for the amplitudes spanning the stable manifold, we have

$$\gamma_{k_1 k_2 l_1 l_2}^{(j)} = \frac{\lambda_{k_1 k_2 l_1 l_2}^{(j11)}}{\sigma_{k_1 k_2}^{(1)} + \sigma_{l_1 l_2}^{(1)} - \sigma_{k_1 + k_2, l_1 + l_2}^{(j)}}. \quad (15)$$

Substitution of (15) into (12) for $A_{\pm 1, 0}^{(1)}$, $A_{0, \pm 1}^{(1)}$, $A_{\pm 1, \pm 1}^{(1)}$, $A_{\pm 2, 0}^{(1)}$, $A_{0, \pm 2}^{(1)}$, and $A_{\pm 2, \pm 2}^{(1)}$ yields twelve-dimensional amplitude equations for themselves. We now simplify the notations by changing $A_{10}^{(1)} \rightarrow z_1$, $A_{01}^{(1)} \rightarrow z_2$, $A_{-1-1}^{(1)} \rightarrow z_3$, $A_{20}^{(1)} \rightarrow z_4$, $A_{02}^{(1)} \rightarrow z_5$, and $A_{-2-2}^{(1)} \rightarrow z_6$. The amplitude equations truncated at the cubic order are obtained as

$$\begin{aligned} \dot{z}_1 &= \sigma_1 z_1 + \delta_1 \bar{z}_2 \bar{z}_3 + \beta_1 \bar{z}_1 z_4 + [\kappa_{11} |z_1|^2 + \kappa_{12} (|z_2|^2 + |z_3|^2)] z_1 \\ &+ [\mu_{11} |z_4|^2 + \mu_{12} (|z_5|^2 + |z_6|^2)] z_1 + \nu_1 \bar{z}_1 \bar{z}_5 \bar{z}_6 + \xi_1 z_2 z_3 z_4 + \eta_1 (\bar{z}_2 z_3 \bar{z}_6 + z_2 \bar{z}_3 \bar{z}_5), \\ \dot{z}_4 &= \sigma_2 z_4 + \delta_2 \bar{z}_5 \bar{z}_6 + \beta_2 z_1^2 + [\kappa_{21} |z_1|^2 + \kappa_{22} (|z_2|^2 + |z_3|^2)] z_4 \\ &+ [\mu_{21} |z_4|^2 + \mu_{22} (|z_5|^2 + |z_6|^2)] z_4 + \nu_2 z_1 \bar{z}_2 \bar{z}_3 + \xi_2 (\bar{z}_3^2 \bar{z}_5 + \bar{z}_2^2 \bar{z}_6), \end{aligned} \quad (16)$$

We set $\sigma_1 = \sigma_{10}^{(1)}$ and $\sigma_2 = \sigma_{20}^{(10)}$. The linear terms $\sigma_1 z_1 = \sigma_{10}^{(1)} z_1$ and $\sigma_2 z_4 = \sigma_{20}^{(1)} z_4$ are retained in (16) although we have already assumed that $\sigma_{10}^{(1)} = \sigma_{20}^{(1)} = 0$ at the very beginning of the above formal analysis. We will change σ_1 and σ_2 as bifurcation parameters, later. The remaining equations for z_2 , z_3 , z_5 , and z_6 are readily obtained by cyclic changes of the subscripts attached to z .

3. Steady solutions and their orbital stability

In this section, we assume that the centre manifold reduction has already been carried out not only up to the cubic order, but up to an arbitrary order of approximation. We first give the general form of the amplitude equations in the presence of the hexagonal lattice symmetry. We then analyze the steady solutions of the amplitude equations and their orbital stability with the aid of the equivariant bifurcation theory. The results of this section are useful when we analyze the steady solutions and their orbital stability for (16), systematically.

The amplitude equations $\dot{z} = g(z, \lambda)$, $g : \mathbf{C}^6 \times \mathbf{R}^2 \rightarrow \mathbf{C}^6$ for

$$z = (z_1(t), z_2(t), z_3(t), z_4(t), z_5(t), z_6(t)) \in \mathbf{C}^6, \quad \lambda \in \mathbf{R}^2 \quad (17)$$

are generated by the vector fields

$$g(z, \lambda) = (g_1(z, \lambda), g_2(z, \lambda), g_3(z, \lambda), g_4(z, \lambda), g_5(z, \lambda), g_6(z, \lambda)). \quad (18)$$

In the presence of a symmetry group Γ , the vector field $g(z, \lambda)$ is said to be equivariant under an action of Γ if

$$g(\gamma z) = \gamma g(z) \quad \text{for all } \gamma \in \Gamma \quad (19)$$

holds. For the hexagonal lattice symmetry, $\Gamma = D_6 \dot{+} T^2$ where D_6 is the dihedral group of the order of six and T^2 is the two-dimensional torus on a plane. For the definition of the semidirect product, see Golubitsky, Stewart and Schaeffer[7], for example.

The dihedral group D_6 is generated by the inversion through the origin

$$c : z \rightarrow \bar{z} \quad (20)$$

and D_3 , which is generated by the counter-clockwise rotation $R_{2\pi/3}$ by the angle $2\pi/3$

$$R_{2\pi/3} : (z_1, z_2, z_3, z_4, z_5, z_6) \rightarrow (z_2, z_3, z_1, z_5, z_6, z_4), \quad (21)$$

and the reflection σ_v in a vertical plane

$$\sigma_v : (z_1, z_2, z_3, z_4, z_5, z_6) \rightarrow (z_1, z_3, z_2, z_4, z_6, z_5). \quad (22)$$

Therefore, eleven non-trivial elements of D_6 send $(z_1, z_2, z_3, z_4, z_5, z_6)$ to

$$\begin{aligned} &(\bar{z}_3, \bar{z}_1, \bar{z}_2, \bar{z}_6, \bar{z}_4, \bar{z}_5), \quad (z_2, z_3, z_1, z_5, z_6, z_4), \quad (\bar{z}_1, \bar{z}_2, \bar{z}_3, \bar{z}_4, \bar{z}_5, \bar{z}_6), \\ &(z_3, z_1, z_2, z_6, z_4, z_5), \quad (\bar{z}_2, \bar{z}_3, \bar{z}_1, \bar{z}_5, \bar{z}_6, \bar{z}_4), \quad (z_1, z_3, z_2, z_4, z_6, z_5), \\ &(z_2, z_1, z_3, z_5, z_4, z_6), \quad (z_3, z_2, z_1, z_6, z_5, z_4), \quad (\bar{z}_3, \bar{z}_2, \bar{z}_1, \bar{z}_6, \bar{z}_5, \bar{z}_4), \\ &(\bar{z}_1, \bar{z}_3, \bar{z}_3, \bar{z}_4, \bar{z}_6, \bar{z}_5), \quad (\bar{z}_2, \bar{z}_1, \bar{z}_3, \bar{z}_5, \bar{z}_4, \bar{z}_6). \end{aligned} \quad (23)$$

The action of $T^2 \subset \Gamma$ is given by

$$(s, t) \cdot z = (e^{is} z_1, e^{-i(s+t)} z_2, e^{it} z_3, e^{2is} z_4, e^{-2i(s+t)} z_5, e^{2it} z_6) \quad (24)$$

for $s, t \in [0, 2\pi)$. See [7] for further details.

The general Γ -equivariant vector field that satisfies $g(\gamma z, \lambda) = \gamma g(z, \lambda)$ for all $\gamma \in \Gamma$ is given by

$$g = g(g_1, g_2, g_3, g_4, g_5, g_6) \quad (25)$$

with

$$\begin{aligned} g_1 &= g_1(z_1, z_2, z_3, z_4, z_5, z_6), \quad g_2 = g_1(z_2, z_3, z_1, z_5, z_6, z_4), \quad g_3 = g_1(z_3, z_1, z_2, z_6, z_4, z_5), \\ g_4 &= g_4(z_1, z_2, z_3, z_4, z_5, z_6), \quad g_5 = g_4(z_2, z_3, z_1, z_5, z_6, z_4), \quad g_6 = g_4(z_3, z_1, z_2, z_6, z_4, z_5). \end{aligned} \quad (26)$$

Here

$$\begin{aligned} g_1(z) &= P_1 z_1 + P_2 \bar{z}_1 z_4 + P_3 \bar{z}_2 \bar{z}_3 + P_4 \bar{z}_1 \bar{z}_5 \bar{z}_6 + P_5 z_2 z_3 z_4 + P_6 \bar{z}_2 z_3 \bar{z}_6 + P_7 z_2 \bar{z}_3 \bar{z}_5 \\ &+ P_8 z_2 z_3 \bar{z}_5 \bar{z}_6 + P_9 z_2 \bar{z}_3 z_4 z_6 + P_{10} \bar{z}_2 z_3 z_4 z_5 + P_{11} \bar{z}_1 \bar{z}_3^2 \bar{z}_5 + P_{12} \bar{z}_1 \bar{z}_2^2 \bar{z}_6, \\ g_4(z) &= Q_1 z_4 + Q_2 z_1^2 + Q_3 \bar{z}_5 \bar{z}_6 + Q_4 z_1 \bar{z}_2 \bar{z}_3 + Q_5 \bar{z}_3^2 \bar{z}_5 + Q_6 \bar{z}_2^2 \bar{z}_6 \\ &+ Q_7 z_1 \bar{z}_2 z_3 \bar{z}_6 + Q_8 z_1 z_2 \bar{z}_3 \bar{z}_5 + Q_9 \bar{z}_2^2 \bar{z}_3^2, \end{aligned} \quad (27)$$

and P_j and Q_j are functions of the invariant polynomials $f(z)$ which satisfies

$$f(\gamma z) = f(z) \quad \text{for all } \gamma \in \Gamma \quad (28)$$

Taylor expanding the P_j and Q_j with respect to the elements of the Γ -invariant polynomials, i.e., the Hilbert basis, and λ about the origin and retaining the leading order terms enable us to see that the cubically truncated amplitude equations generated by (25) agrees with (16), formally. This guarantees that no other terms are possible to be added in (16) at the cubic order approximation.

We now classify the steady-state solutions of the amplitude equations $\dot{z} = g(z, \lambda)$. We need to recall some fundamentals which are borrowed from [7].

Table 2. Branching equations truncated at the cubic order. $\dim \text{Fix}(\Sigma) \leq 2$.

Label	Nomenclature	Branching equations
2	Simple Roll	$\sigma_2 + \mu_{21}x^2 = 0$
3	Simple Hexagon	$\sigma_2 + \delta_2x + (\mu_{21} + 2\mu_{22})x^2 = 0$
4	Super Roll	$\sigma_1 + \beta_1y + \kappa_{11}x^2 + \mu_{11}y^2 = 0,$ $\sigma_2y + \beta_2x^2 + \kappa_{21}x^2y + \mu_{21}y^3 = 0$
5	Simple Rectangle	$\sigma_2x + \delta_2y^2 + (\mu_{21}x^2 + 2\mu_{22}y^2)x = 0,$ $\sigma_2 + \delta_2x + \mu_{22}x^2 + (\mu_{21} + \mu_{22})y^2 = 0$
6	Super Hexagon	$\sigma_1 + \beta_1y + \delta_1x + (\kappa_{11} + 2\kappa_{12})x^2 + (\mu_{11} + 2\mu_{12} + \nu_1)y^2$ $+ (2\eta_1 + \xi_1)xy = 0,$ $\sigma_2y + \beta_2x^2 + \delta_2y^2 + (\kappa_{21} + 2\kappa_{22} + 2\xi_2)x^2y$ $+ (\mu_{21} + 2\mu_{22})y^3 + \nu_2x^3 = 0$
7	Triangle	$\sigma_2x + \delta_2(x^2 - y^2) + (\mu_{21} + 2\mu_{22})x^3 + (\mu_{21} + 2\mu_{22})xy^2 = 0,$ $\sigma_2 - 2\delta_2x + (\mu_{21} + 2\mu_{22})x^2 + (\mu_{21} + 2\mu_{22})y^2 = 0$

If z is a point of \mathbf{C}^6 , the elements of Γ which leave z fixed form a subgroup of Γ called the isotropy subgroup or stabilizer Σ_z defined by

$$\Sigma_z = \{\sigma \in \Gamma : \sigma z = z\} \quad (29)$$

The fixed point subspace of a subgroup $\Sigma \subset \Gamma$ is given by

$$\text{Fix}(\Sigma) = \{z \in \mathbf{C}^6 : \sigma z = z \text{ for all } \sigma \in \Sigma\}. \quad (30)$$

Points on the same orbit of Γ , i.e., $\Gamma z = \{\gamma z : \gamma \in \Gamma, z \in \mathbf{C}^6\}$, have conjugate isotropy subgroups,

$$\Sigma_{\gamma z} = \gamma \Sigma_z \gamma^{-1}. \quad (31)$$

We thus classify the isotropy subgroups up to conjugacy classes.

Table 1 lists the fixed points of $g(z, \lambda) = 0$ and the isotropy subgroups of Γ acting on \mathbf{C}^6 together with their fixed point subspaces. In the table,

$$\begin{aligned} S^1(0, \theta) &: (z_1, z_2, z_3, z_4, z_5, z_6) \rightarrow (z_1, z_2 e^{-i\theta}, z_3 e^{i\theta}, z_4, z_5 e^{-2i\theta}, z_6 e^{2i\theta}), \\ Z_2(\pi, 0) &: (z_1, z_2, z_3, z_4, z_5, z_6) \rightarrow (-z_1, -z_2, z_3, z_4, z_5, z_6), \\ Z_2(0, \pi) &: (z_1, z_2, z_3, z_4, z_5, z_6) \rightarrow (z_1, -z_2, -z_3, z_4, z_5, z_6). \end{aligned} \quad (32)$$

There are two primary branches, i.e., type 2 and 3 solutions. The simple roll and simple hexagonal pattern possess the wavenumber $2k_c$. Since we assume the generic situation without degeneracy, neither the rolls with k_c nor the hexagons with k_c may exist. Four secondary branches satisfying $\dim \text{Fix}(\Sigma) = 2$ may exist; they are type 4, 5, 6, and 7 solutions. As is seen from the Table 1, super-rolls are composed of rolls with wavenumber k_c and rolls with $2k_c$.

Likewise, super-hexagons are composed of hexagons with wavenumber k_c and hexagons with $2k_c$.

The cubic truncation of the branching equations are listed in Table 2 for $\dim \text{Fix}(\Sigma) \leq 2$. For type 7 solution, we set $z = x + iy$ with $x, y \in \mathbf{R}$.

Let us now evaluate the orbital stability of the fixed points of Table 1. We compute the eigenvalues of the Jacobian matrices in terms of the general form of the amplitude equations generated by the Γ -equivariant vector field, $\dot{z} = g(z, \lambda)$, where $z \in \mathbf{C}^6$ and $g : \mathbf{C}^6 \times \mathbf{R}^2 \rightarrow \mathbf{C}^6$.

Since the vector field g is Γ -equivariant, we have $g(\gamma z, \lambda) = \gamma g(z, \lambda)$ for all $\gamma \in \Gamma$. The Jacobian matrix dg about the fixed point $z = z_0$ thus needs to satisfy

$$dg(\gamma z_0, \lambda)\gamma = \gamma dg(z_0, \lambda). \quad (33)$$

If $\gamma \in \Sigma_z \subset \Gamma$, we replace γ with $\sigma \in \Sigma_{z_0}$, and we have

$$dg(z_0, \lambda)\sigma = \sigma dg(z_0, \lambda). \quad (34)$$

By x_j, y_j and g_j^r, g_j^i , we denote the real and the imaginary parts of z_j and g_j for $1 \leq j \leq 6$:

$$z_j = x_j + iy_j; \quad g_j = g_j^r + ig_j^i. \quad (35)$$

The Jacobian matrix $dg(z_0, \lambda)$ is thus 12×12 and real. The commutativity relation (34) enables us to compute the eigenvalues of $dg(z_0, \lambda)$ directly for relatively low dimensional $\text{Fix}(\Sigma)$.

Let $\gamma(\theta)$ be a smooth curve in Γ and $\gamma(0) = 1$. Since $g(z_0) = 0$, the Γ -equivariance implies that

$$g(\gamma(\theta)z_0) = 0. \quad (36)$$

Differentiating (36) with respect to θ and evaluating at $\theta = 0$ yield

$$dg(z_0) \frac{\partial \gamma}{\partial \theta} \Big|_{\theta=0} \cdot z_0 = 0. \quad (37)$$

Equation (37) shows that $\frac{\partial \gamma}{\partial \theta} \Big|_{\theta=0} \cdot z_0$ is an eigenvector of $dg(z_0)$ belonging to the zero eigenvalue.

Details of the computation of the eigenvalues are omitted but the results for solutions with $\dim \text{Fix}(\Sigma) \leq 2$ are summarized on Table 3. It is obvious from Table 3 that the Hopf bifurcation may occur on type 4, 5, 6, and 7 solution branches. On type 2 and 3 solution branches, only steady bifurcations arise.

Table 4 shows the signs of the eigenvalues at the cubic order approximation and eigenvectors belonging to the eigenvalues for type 2 and 3 solutions. On the type 2 solution branch, type 4 solution bifurcates at $\frac{\partial g_1^r}{\partial x_1} = 0$ and $\frac{\partial g_1^i}{\partial y_1} = 0$, type 5 solution bifurcates at $\frac{\partial g_5^r}{\partial x_5} \pm \frac{\partial g_5^i}{\partial x_6} = 0$. Supercriticality of the type 2 solution is guaranteed if $\frac{\partial g_4^r}{\partial x_4} < 0$ holds. If $\frac{\partial g_2^r}{\partial x_2} = 0$ holds, linear combinations of the four eigenvectors may create type 12, 13, 16, 17, 18, or 19 solutions in principle.

Supercriticality of the type 3 solution is guaranteed if $\frac{\partial g_4^r}{\partial x_4} + 2\frac{\partial g_4^r}{x_5} < 0$ holds. On the type 3 solution branch, type 7 solution bifurcates at $\frac{\partial g_4^i}{\partial y_4} = 0$, type 5 solution bifurcates at $\frac{\partial g_4^r}{\partial x_4} - \frac{\partial g_5^r}{\partial x_5} = 0$, type 6 and 8 solutions may bifurcate at $\frac{\partial g_1^r}{\partial x_1} = 0$, and type 11, 12, 14, or 17 solutions may bifurcate at $\frac{\partial g_1^i}{\partial y_1} = 0$.

Note that the orbital stability determined in this paper is with respect to disturbances supported only by the hexagonal lattice and not by a different lattice like the square or the rectangular.

4. Application to two-layered Rayleigh-Bénard convection

4.1. Governing equations and numerical methods

In this section, we apply the above analyses to the Rayleigh-Bénard convection composed of two horizontal fluid layers. They are sandwiched between a top and a bottom horizontal plates and a horizontal ‘splitter plate’ which is non-deformable, conducting, and thin. The bottom plate is heated and the top plate is cooled at different but uniform temperatures. Because of the splitter plate, there is no mechanical coupling between the upper and the lower fluid layers. The convection of this type was found by Proctor and Jones to have the possibility that the exact 2:1 resonance takes place between the critical modes. They analyzed the bifurcation in one-dimensional 2:1 resonance, in detail, based on the cubically truncated equations (3). In the one-dimensional pattern formation problem, the cubic amplitude equations describing the 2:1 resonance (3) are generic. However, since the linear operators of the problem, \mathcal{S} and \mathcal{L} , are self-adjoint, the cubic amplitude equations (16) are not generic for two-dimensional pattern formation problem: the coefficients δ_1 and δ_2 of the quadratic nonlinear terms vanish[11]. In order to make the cubic equations generic, we need to violate the self-adjointness of the operators. In this section, we do so by assuming the quadratic density profiles as functions of the temperature.

We take the horizontal co-ordinates x^* and y^* , and the vertical co-ordinate z^* which is opposite to the direction of the gravity. In what follows, all the asterisked quantities are dimensional. The bottom and the top plates are located at $z^* = 0$ and $d(1 + D^{-1})$, respectively, and the splitter plate is located at $z^* = d$. The temperatures on the bottom and the top plates are maintained at $T^* = T_b$ and T_t^* , respectively. The temperature on the splitter plate is at $T^* = T_m$.

We attach suffixes 1 and 2 to indicate variables and physical properties in the lower layer and the upper layer, respectively. The governing equations for the velocities $\vec{v}_{1,2}^*$, the pressures $p_{1,2}^*$, and the temperatures $T_{1,2}^*$ are given by

$$\begin{aligned} \rho_0^{(1)} \frac{D\vec{v}_1^*}{Dt^*} &= -\nabla^* p_1^* - \rho_0^{(1)} g [1 - \alpha_1^{(1)} (T_1^* - T_m) - \alpha_2^{(1)} (T_1^* - T_m)^2] \mathbf{e}_z + \mu_1 \Delta^* \vec{v}_1^*, \\ \rho_0^{(2)} \frac{D\vec{v}_2^*}{Dt^*} &= -\nabla^* p_2^* - \rho_0^{(2)} g [1 - \alpha_1^{(2)} (T_2^* - T_m) - \alpha_2^{(2)} (T_2^* - T_m)^2] \mathbf{e}_z + \mu_2 \Delta^* \vec{v}_2^*, \\ \frac{DT_1^*}{Dt^*} &= \kappa_1 \Delta^* T_1^*, \quad \frac{DT_2^*}{Dt^*} = \kappa_2 \Delta^* T_2^*, \\ \nabla^* \cdot \vec{v}_1^* &= 0, \quad \nabla^* \cdot \vec{v}_2^* = 0. \end{aligned} \tag{38}$$

Here, g is the acceleration due to the gravity, $\mu_{1,2}$ are the viscous coefficients, $\kappa_{1,2}$ are the thermal diffusivities, and $\rho_0^{(1)}$ and $\rho_0^{(2)}$ are the densities of the fluids at $T_1^* = T_m$ and $T_2^* = T_m$, respectively. In (38), we assumed that the Bussinesq approximation holds for the upper and the lower fluids so that the densities only in the buoyancy terms are functions of the temperature. In the buoyancy terms, $\alpha_{1,2}^{(1)}$ and $\alpha_{1,2}^{(2)}$ are thermal expansion coefficients. If $\alpha_2^{(1)} = \alpha_2^{(2)} = 0$, the linear operators are self-adjoint.

Let us now non-dimensionalize (38) by setting

$$t^* = \frac{d^2}{\kappa_1} t, \quad \vec{v}_1^* = \frac{\kappa_1}{d} \vec{v}_1, \quad \vec{v}_2^* = \frac{\kappa_1}{d} \vec{v}_2, \quad \vec{x}^* = d \vec{x},$$

$$\begin{aligned}
p_1^* &= -d\rho_0^{(1)}g \int^z [1 - \alpha_1^{(1)}(T_b - T_m)(1 - z) - \alpha_2^{(1)}(T_b - T_m)^2(1 - z)^2]dz + \rho_0^{(1)}\frac{\kappa_1^2}{d^2}\pi_1, \\
p_2^* &= -d\rho_0^{(2)}g \int^z [1 - \alpha_1^{(2)}(T_m - T_t)D(1 - z) - \alpha_2^{(2)}(T_m - T_t)^2D^2(1 - z)^2]dz + \rho_0^{(2)}\frac{\kappa_1^2}{d^2}\pi_2, \\
T_1^* - T_m^* &= (T_b - T_m)[(1 - z) + \theta_1(x, y, z; t)], \quad z \in [0, 1], \\
T_2^* - T_m^* &= (T_m - T_t)D[(1 - z) + \theta_2(x, y, z; t)], \quad z \in [1, 1 + D^{-1}].
\end{aligned} \tag{39}$$

We define non-dimensional parameters by

$$\begin{aligned}
R_1 &= \frac{\rho_0^{(1)}g\alpha_1^{(1)}(T_b - T_m)d^3}{\mu_1\kappa_1}, \quad R_2 = \frac{\rho_0^{(2)}g\alpha_1^{(2)}(T_m - T_t)d^3}{D^3\mu_2\kappa_2}, \quad P_1 = \frac{\nu_1}{\kappa_1}, \quad P_2 = \frac{\nu_2}{\kappa_2}, \\
C_1 &= 1, \quad C_2 = \frac{\kappa_1}{\kappa_2}, \quad K_1 = 1, \quad K_2 = D^4, \quad \epsilon_1 = \frac{\alpha_2^{(1)}(T_b - T_m)}{\alpha_1^{(1)}}, \quad \epsilon_2 = \frac{\alpha_2^{(2)}(T_m - T_t)D}{\alpha_1^{(2)}}.
\end{aligned} \tag{40}$$

Following Proctor and Jones, we assume $C_2 = 1$. We further set $\bar{T} = 1 - z$. The disturbance equations in non-dimensional form are written as

$$\begin{aligned}
P_1^{-1}\frac{D\vec{v}_1}{Dt} &= -P_1^{-1}\nabla\pi_1 + R_1K_1\theta_1\mathbf{e}_z + R_1K_1\epsilon_1(2\bar{T}\theta_1 + \theta_1^2)\mathbf{e}_z + \Delta\vec{v}_1, \\
P_2^{-1}\frac{D\vec{v}_2}{Dt} &= -P_2^{-1}\nabla\pi_2 + R_2K_2\theta_2\mathbf{e}_z + R_2K_2\epsilon_2(2\bar{T}\theta_2 + \theta_2^2)\mathbf{e}_z + \Delta\vec{v}_2, \\
\frac{D\theta_1}{Dt} - w_1 &= \Delta\theta_1, \quad \frac{D\theta_2}{Dt} - w_2 = \Delta\theta_2, \\
\nabla \cdot \vec{v}_1 &= 0, \quad \nabla \cdot \vec{v}_2 = 0.
\end{aligned} \tag{41}$$

Here, $\vec{v}_{1,2} = (u_{1,2}, v_{1,2}, w_{1,2})^T$.

We impose the boundary conditions

$$\begin{aligned}
\vec{v}_1 = \vec{v}_2 &= 0 \quad \text{at } z = 0, 1, 1 + D^{-1}, \\
\theta_1 = \theta_2 &= 0 \quad \text{at } z = 0, 1 + D^{-1}.
\end{aligned} \tag{42}$$

The boundary conditions at $z = 1$ for the temperature are imposed by

$$T_1^* = T_2^*, \quad \kappa_1\frac{dT_1^*}{dz^*} = \kappa_2\frac{dT_2^*}{dz^*}, \tag{43}$$

which yield

$$\theta_1 = \frac{R_2}{R_1}\frac{D^4\alpha_1^{(1)}\nu_2\kappa_2}{\alpha_1^{(2)}\nu_1\kappa_1}\theta_2 \equiv G\theta_2, \quad \frac{d\theta_1}{dz} = G\frac{d\theta_2}{dz} \quad \text{at } z = 1. \tag{44}$$

Eliminating the pressure terms, we obtain the disturbance equations as

$$\begin{aligned}
\left(\frac{\partial}{\partial t} - P_j\Delta\right)\left(\frac{\partial v_j}{\partial x} - \frac{\partial u_j}{\partial y}\right) &= \frac{\partial}{\partial x}(\vec{v}_j \cdot \nabla)v_j - \frac{\partial}{\partial y}(\vec{v}_j \cdot \nabla)u_j, \\
P_j^{-1}\frac{\partial\Delta w_j}{\partial t} - \Delta^2 w_j - R_jK_j\Delta_2\theta_j - 2\epsilon_jR_jK_j\Delta_2(\bar{T}\theta_j) \\
&= P_j^{-1}\left[\frac{\partial^2}{\partial x\partial z}(\vec{v}_j \cdot \nabla)u_j + \frac{\partial^2}{\partial y\partial z}(\vec{v}_j \cdot \nabla)v_j - \Delta_2(\vec{v}_j \cdot \nabla)w_j\right] + \epsilon_jR_jK_j\Delta_2\theta_j^2,
\end{aligned}$$

$$\begin{aligned}\frac{\partial \theta_j}{\partial t} - \Delta \theta_j - w_j &= -(\vec{v}_j \cdot \nabla) \theta_j, \\ \nabla \cdot \vec{v}_j &= 0,\end{aligned}\tag{45}$$

where $\Delta_2 = \frac{\partial^2}{\partial x^2} + \frac{\partial^2}{\partial y^2}$ is the horizontal Laplacian.

Introduce the normal mode

$$(u_j, v_j, w_j, \theta_j)^T = (\hat{u}_j, \hat{v}_j, \hat{w}_j, \hat{\theta}_j) e^{\sigma t + i(\alpha x + \beta y)}.\tag{46}$$

The linear eigenvalue problem thus consists of

$$\begin{aligned}P_j^{-1} \sigma (i\alpha v_j - i\beta u_j) - \mathcal{S}(i\alpha v_j - i\beta u_j) &= 0, \\ i\alpha u_j + i\beta v_j + \mathcal{D}w_j &= 0, \\ P_j^{-1} \sigma \mathcal{S}w_j - \mathcal{S}^2 w_j + R_j K_j \gamma^2 \theta_j + 2\epsilon_j R_j K_j \gamma^2 \bar{T} \theta_j &= 0, \\ \sigma \theta_j - \mathcal{S} \theta_j - w_j &= 0\end{aligned}\tag{47}$$

under

$$\begin{aligned}u_j = v_j = w_j = \mathcal{D}w_j = \theta_j = 0 \text{ at } z = 0, 1 + D^{-1}, \\ u_j = v_j = w_j = \mathcal{D}w_j = 0, \theta_1 = G\theta_2, \mathcal{D}\theta_1 = G\mathcal{D}\theta_2 \text{ at } z = 1.\end{aligned}\tag{48}$$

Here, \mathcal{D} denotes $\frac{d}{dz}$.

We solved the linear eigenvalue problem (47) and (48) and corresponding adjoint problem by means of the expansions in Chebyshev polynomials. The boundary conditions at $z = 1$ are imposed by the tau method. An application of the collocation method yields algebraic eigenvalue problems. The QZ package of IMSL is used to solve the problems, numerically. First, we confirmed the accuracy of the resonance conditions which are given in Table 1 of Proctor and Jones; i.e., $R_1 = 1401.8$, $r \equiv R_2/R_1 = 1.0607$, $k_c = \sqrt{\alpha^2 + \beta^2} = 2.9150$, and $D = 2.0977$ for the linear density profile with $\alpha_2^{(1)} = \alpha_2^{(2)} = 0$. In Fig.1, we show the linear neutral curves for two Prandtl number sets, $(P_1, P_2) = (7, 7)$ and $(143.759, 7)$ with various values of ϵ_1 and ϵ_2 . We have fixed the value of the depth ratio as $D = 2.0977$ which is the same as the one reported in Proctor and Jones. The linear neutral stability curves exhibit the exact 2:1 resonance. Two minima on the curves having wavenumbers in the ratio 2:1 give exactly the same critical Rayleigh numbers. The exact resonance for various ϵ_1 and ϵ_2 values is not surprising since the resonance has already existed for $\epsilon_1 = \epsilon_2 = 0$.

All the eigenfunctions and the adjoint functions are normalized such that $\langle \vec{\psi}_{mn}^{(j)}, \mathcal{S}\psi_{mn}^{(j)} \rangle = 1$. After computing $\sigma_{mn}^{(j)}$ and $\lambda_{k,l,m-k,n-l}^{(1,p,q)}$ in (12), we evaluated all the coefficients involved in (16) numerically both for $P_1 = P_2 = 7$ and $P_1 = 143.759$ and $P_2 = 7$ and tabulated the results in Table 5 and 6, respectively. In the evaluation, we assumed that the depth ratio D takes the value 2.0977. From our numerical data, we found that $k_c \simeq 2.9150$ gives the 2:1 resonance for all the cases shown in the tables. In order to obtain the results, we truncated the expansions in Chebyshev polynomials at the 30-th degree and the expansion in the linear eigenfunctions at the 20-th.

Since the linear operators involved in our problem for $\epsilon_1 = \epsilon_2 = 0$ are self-adjoint, the numerical values of δ_1 and δ_2 vanish in Tables 5 and 6. We may see how they recover non-vanishing values when ϵ_1 and ϵ_2 deviates from $(0, 0)$. Slight increase of the value of ϵ_2 causes significant effect on the non-self-adjointness.

4.2. Bifurcation diagrams

Based upon the numerical data of Table 5 for $\epsilon_1 = \epsilon_2 = 0.1$ and Table 6 for $\epsilon_1 = 0$ and $\epsilon_2 = 0.1$, let us examine the bifurcation characteristics of the steady solutions of (16). The resonance considered is a two-parameter bifurcation problem. In our amplitude equations, two linear growth rates, σ_1 and σ_2 are formally retained although they are assumed to vanish at the linear criticality. In general, they depend on physical parameters such as $R_1, R_2/R_1, P_1, P_2, D$, etc. In the present paper, we regard σ_1 and σ_2 as the bifurcation parameters, for simplicity. Let us set

$$\sigma_1 = \epsilon \cos \varphi, \quad \sigma_2 = \epsilon \sin \varphi,$$

where φ lies in $[0, 2\pi]$. The modulus ϵ is set to be 10^{-4} . This value is so small that the steady solutions obtained may be considered to be local.

In Figs.2 and 3, only the primary and the secondary solution branches are depicted. The bifurcation points are shown by the closed circles on the steady solution branches whose $\dim \text{Fix}(\Sigma) \leq 2$. For the stability of each solution branch, see Tables 7 and 8. The stability assignments of the tables are such that “+” denotes a positive eigenvalues, “-” denotes a negative eigenvalue, “* *” denotes a pair of conjugate complex eigenvalues whose real parts are positive, “==” denotes a pair of conjugate complex eigenvalues whose real parts are negative, and “0” denotes a zero eigenvalue forced by the symmetry.

Each entry in Tables 7 and 8 respectively corresponds to the eigenvalues listed in Table 3. Since the information about the multiplicity of a degenerate eigenvalue is involved in Table.3, we ignored them in Tables 7 and 8. As the primary solutions, both type 2 and 3 solutions bifurcate from the trivial solution at $\varphi = 0, \pi$, and 2π . The type 2 solution exists in $0 \leq \varphi \leq \pi$ while the type 3 solutions exist in $0 \leq \varphi \leq \pi$ and $\pi \leq \varphi \leq 2\pi$. Since we are looking at the local steady solutions with small norm, another type 3 solution branch with large norm does not appear in the figures although they do exist for $0 \leq \varphi \leq 2\pi$. The existence ranges of these primary solutions are entirely consistent with the existence ranges of rolls and hexagons in pattern formation problems without resonance (see Fig.1a in Buzano and Golubitsky, for instance). Because of the 2:1 resonant interaction, the third branch of the type 3 solutions cannot be stable in both figures. The stability of the third branch is given by “--0-+-” everywhere as far as (σ_1, σ_2) is in the neighborhood of the origin. The positive eigenvalue $\frac{\partial g_1^r}{\partial x_1}$ has multiplicity three. Table 4 shows that the eigenvectors belonging to $\frac{\partial g_1^r}{\partial x_1}$ involve one of non-vanishing x_1, x_2 , and x_3 where $x_1, x_2, x_3 \in \mathbf{R}$.

Let us now discuss about the stability of the primary solutions and the secondary bifurcations from them in Fig.2. Type 2 solution is unstable as is listed in Table 7. On the type 2 solution branch, three bifurcation points exist. At the bifurcation points, at least one eigenvalue needs to change the sign of its real part. For example, the sign of $\frac{\partial g_1^i}{\partial y_1}$ changes at $\varphi \simeq 5 \times 10^{-5}\pi$ at which the stability assignment changes from 2a to 2b with the increase of φ . By “(7cd)”, let us denote a bifurcation point at which the stability assignment changes from 7c to 7d, for example, for later convenience. At bifurcation point (2ab), type 4 solution having a property $2\arg(z_1) - \arg(z_4) = (2n+1)\pi$, ($n = 0, \pm 1, \dots$) bifurcates. It vanishes at $\varphi = 3\pi/2$ on the trivial solution. This corresponds to “S-” of [5] or “M-” of [1] and [10]. At point (2cd), $\frac{\partial g_1^r}{\partial x_1}$ changes its sign and another type 4 solution with $2\arg(z_1) - \arg(z_4) = 2n\pi$ bifurcates. The latter type 4 solution branch vanishes at $\varphi = \pi/2$ on the trivial solution. It corresponds to “S+” or “M+”. At bifurcation point (2bc), $\frac{\partial g_2^r}{\partial x_2}$ vanishes. This eigenvalue is degenerate with multiplicity four

as has been listed in Table 4. At most four solution branches are thus expected to bifurcate; at this moment, three bifurcating branches are identified, i.e., two type 12 solutions and one type 13 solution.

On the type 3 solution branch, twelve branches bifurcate in total. As is seen from Tables 7 and 3, $\frac{\partial g_1^r}{\partial x_1}$ changes its sign at (3ab) and (3de) while $\frac{\partial g_1^i}{\partial y_1}$ changes its sign at (3bc) and (3ef). These eigenvalues are degenerate with multiplicity three. At most three branches are thus expected to bifurcate at each bifurcation points. Two type 6 solutions and type 12 solution bifurcate at (3ab) and (3de) whereas type 8, type 11, and type 12 solutions bifurcate at (3bc) and (3ef). The type 6 solutions are two-dimensional extension of type 4 solutions.

We have identified the primary and the secondary branches and examined the orbital stability of the type 4 and 6 solutions whose $\dim \text{Fix}(\Sigma) = 2$. Although we do not involve the detailed information about the signs of the eigenvalues for secondary solutions with $\dim \text{Fix}(\Sigma) \geq 3$, we need to note that they are orbitally unstable. In summary, only the short segment 6i' is orbitally stable.

Figure 3 shows similar bifurcation diagram for $P_1 = 143.759$, $P_2 = 7$, $\epsilon_1 = 0$, and $\epsilon_2 = 0.1$. For the stability of the primary and the secondary solution branches with $\dim \text{Fix}(\Sigma) \leq 2$, see Table 8. Again, a small segment on the type 6 solution is found to be unstable. All the other primary and the secondary branches shown in the figure are found to be unstable.

References

- [1] Armbruster D., Guckenheimer J., P. Holmes, Heteroclinic cycles and modulated traveling waves in systems with $O(2)$ symmetry, *Physica D* **29** (1988) 257–282.
- [2] E. Buzano, M. Golubitsky, Bifurcation on the hexagonal lattice and the planar Bénard problem, *Phil. Trans. R. Soc. Lond.* **A308** (1983) 617–667.
- [3] E. Buzano, A. Russo, Bifurcation problems with $O(2) \oplus Z_2$ symmetry and the buckling of a cylindrical shell, *Annali di Matematica Pura ed Applicata (IV)* **146** (1987) 217–262.
- [4] J. Carr, *Applications of Centre Manifold Theory*, (Springer-Verlag, 1981).
- [5] G. Dangelmayr, Steady state mode interactions in presence of $O(2)$ symmetry, *Dyn. Stab. Syst.* **1** (1986) 159–185.
- [6] K. Fujimura, Centre manifold reduction and the Stuart-Landau equation for fluid motions, *Proc. R. Soc. Lond.* **A453** (1997) 181–203.
- [7] M. Golubitsky, I. Stewart, D.G. Shaeffer, *Singularities and Groups in Bifurcation Theory, volume II*, (Springer-Verlag, 1988).
- [8] M. Golubitsky, J.W. Swift, E. Knobloch, Symmetries and pattern selection in Rayleigh-Bénard convection, *Physica D* **10** (1984) 249–276.
- [9] J. Porter, E. Knobloch, New type of complex dynamics in the 1:2 spatial resonance.
- [10] M.R.E. Proctor, C.A. Jones, The interaction of two spatially resonant patterns in thermal convection. Part 1. Exact 1:2 resonance, *J. Fluid Mech.* **188**, (1988) 301–335.
- [11] A. Schlüter, D. Lortz, F.H. Busse, On the stability of steady finite amplitude convection, *J. Fluid Mech.* **23** (1965) 129–144.

Table 1. The orbit representatives and the isotropy subgroups of the fixed points under $D_6 \dot{+} T^2$

Label	Orbit Representative	Σ_z	Generators of Σ_z	$\text{Fix}(\Sigma_z)$	$\dim \text{Fix}(\Sigma_z)$
1	$(0,0,0,0,0,0)$	$D_6 \dot{+} T^2$	$R_{2\pi/3}, c, c_v, S^1(\theta, 0), S^1(0, \theta)$		
2	$(0,0,0,x,0,0)$ $x \in \mathbf{R}$	$S^1 + Z_2^3$	$c, c_v, Z_2(\pi, 0), S^1(0, \theta)$	$\mathbf{R}\{(0,0,0,1,0,0)\}$	1
3	$(0,0,0,x,x,x)$ $x \in \mathbf{R}$	$D_6 + Z_2^2$	$R_{2\pi/3}, c, c_v, Z_2(\pi, 0), Z_2(0, \pi)$	$\mathbf{R}\{(0,0,0,1,1,1)\}$	1
4	$(x,0,0,y,0,0)$ $x, y \in \mathbf{R}$	$S^1 + Z_2^2$	$c, c_v, S^1(0, \theta)$	$\mathbf{R}\{(1,0,0,0,0,0), (0,0,0,1,0,0)\}$	2
5	$(0,0,0,x,y,y)$ $x=y \in \mathbf{R}$	Z_2^4	$c, c_v, Z_2(\pi, 0), Z_2(0, \pi)$	$\mathbf{R}\{(0,0,0,1,0,0), (0,0,0,0,1,1)\}$	2
6	(x,x,x,y,y,y) $x,y \in \mathbf{R}$	D_6	$R_{2\pi/3}, c, c_v$	$\mathbf{R}\{(1,1,1,0,0,0), (0,0,0,1,1,1)\}$	2
7	$(0,0,0,z,z,z)$ $z \in \mathbf{C}$	$D_3 + Z_2^2$	$R_{2\pi/3}, c_v, Z_2(\pi, 0), Z_2(0, \pi)$	$\mathbf{C}\{(0,0,0,1,1,1)\}$	2
8	$(z,0,0,x,y,y)$ $z, x=y \in \mathbf{R}$	Z_2^3	$c, c_v, Z_2(0, \pi)$	$\mathbf{R}\{(1,0,0,0,0,0), (0,0,0,1,0,0), (0,0,0,0,1,1)\}$	3
9	$(0,0,0,x,y,z)$ $x=y=z \in \mathbf{R}$	Z_2^3	$c, Z_2(\pi, 0), Z_2(0, \pi)$	$\mathbf{R}\{(0,0,0,1,0,0), (0,0,0,0,1,0), (0,0,0,0,0,1)\}$	3
10	$(0,0,0,x,y,y)$ $x \in \mathbf{C}, y \in \mathbf{R}$	Z_2^3	$c_v, Z_2(\pi, 0), Z_2(0, \pi)$	$\mathbf{R}\{(0,0,0,1,0,0), (0,0,0,i,0,0), (0,0,0,0,1,1)\}$	3
11	(x,x,x,y,y,y) $x,y \in \mathbf{C}$	D_3	$R_{2\pi/3}, c_v$	$\mathbf{C}\{(1,1,1,0,0,0), (0,0,0,1,1,1)\}$	4
12	$(x_1, x_2, x_2, y_1, y_2, y_2)$ $x_1 = x_2, y_1 = y_2 \in \mathbf{R}$	Z_2^2	c, c_v	$\mathbf{R}\{(1,0,0,0,0,0), (0,1,1,0,0,0), (0,0,0,1,0,0), (0,0,0,0,1,1)\}$	4
13	$(x,0,0,y_1, y_2, y_3)$ $x, y_1 = y_2 = y_3 \in \mathbf{R}$	Z_2^2	$c, Z_2(0, \pi)$	$\mathbf{R}\{(1,0,0,0,0,0), (0,0,0,1,0,0), (0,0,0,0,1,0), (0,0,0,0,0,1)\}$	4
14	$(z,0,0,x,y,y)$ $x=y, z \in \mathbf{C}$	Z_2^2	$c_v, Z_2(0, \pi)$	$\mathbf{C}\{(1,0,0,0,0,0), (0,0,0,1,0,0), (0,0,0,0,1,1)\}$	6
15	$(0,0,0,x,y,z)$ $x=y=z \in \mathbf{C}$	Z_2^2	$Z_2(\pi, 0), Z_2(0, \pi)$	$\mathbf{C}\{(0,0,0,1,0,0), (0,0,0,0,1,0), (0,0,0,0,0,1)\}$	6
16	$(x_1, x_2, x_3, y_1, y_2, y_3)$ $x_1 = x_2 = x_3, y_1 = y_2 = y_3 \in \mathbf{R}$	Z_2	c	\mathbf{R}^6	6
17	$(x_1, x_2, x_2, y_1, y_2, y_2)$ $x_1 = x_2, y_1 = y_2 \in \mathbf{C}$	Z_2	c_v	$\mathbf{C}\{(1,0,0,0,0,0), (0,1,1,0,0,0), (0,0,0,1,0,0), (0,0,0,0,1,1)\}$	8
18	$(w,0,0,x,y,z)$ $w, x=y=z \in \mathbf{C}$	Z_2	$Z_2(0, \pi)$	$\mathbf{C}\{(1,0,0,0,0,0), (0,0,0,1,0,0), (0,0,0,0,1,0), (0,0,0,0,0,1)\}$	8
19	$(x_1, x_2, x_3, y_1, y_2, y_3)$ $x_1 = x_2 = x_3, y_1 = y_2 = y_3 \in \mathbf{C}$	$\{1\}$	1	\mathbf{C}^6	12

Table 3. Eigenvalues of the Jacobian matrices for the primary and the secondary solutions.

Label	Eigenvalues	Multiplicity
1	$\frac{\partial g_1^r}{\partial x_1}, \frac{\partial g_4^r}{\partial x_4}$	6,6
2	$0, \frac{\partial g_1^r}{\partial x_1}, \frac{\partial g_1^i}{\partial y_1}, \frac{\partial g_4^r}{\partial x_4}$	1,1,1,1
	$\frac{\partial g_5^r}{\partial x_5} + \frac{\partial g_5^i}{\partial x_6}, \frac{\partial g_5^r}{\partial x_5} - \frac{\partial g_5^i}{\partial x_6}$	2,2
	$\frac{\partial g_2^r}{\partial x_2}$	4
3	$\frac{\partial g_4^r}{\partial x_4} + 2\frac{\partial g_4^r}{\partial x_5}, 3\frac{\partial g_4^i}{\partial y_4}$	1,1
	$0, \frac{\partial g_4^r}{\partial x_4} - \frac{\partial g_4^r}{\partial x_5}$	2,2
	$\frac{\partial g_1^r}{\partial x_1}, \frac{\partial g_1^i}{\partial y_1}$	3,3
4	$0, \frac{\partial g_1^i}{\partial y_1} + \frac{\partial g_4^i}{\partial y_4}$	1,1
	$\frac{\partial g_5^r}{\partial x_5} - \frac{\partial g_5^i}{\partial x_6}, \frac{\partial g_5^r}{\partial x_5} + \frac{\partial g_5^i}{\partial x_6}, \frac{\partial g_2^r}{\partial x_2} - \frac{\partial g_2^i}{\partial x_3}, \frac{\partial g_2^r}{\partial x_2} + \frac{\partial g_2^i}{\partial x_3}$	2,2,2,2
	$\lambda_1^{(4)}, \lambda_2^{(4)}; \lambda_1^{(4)} + \lambda_2^{(4)} = \text{tr } A, \lambda_1^{(4)}\lambda_2^{(4)} = \det A, A = \begin{pmatrix} \frac{\partial g_1^r}{\partial x_1} & \frac{\partial g_1^r}{\partial x_4} \\ \frac{\partial g_4^r}{\partial x_1} & \frac{\partial g_4^r}{\partial x_4} \end{pmatrix}$	1,1
5	$\frac{\partial g_1^r}{\partial x_1}, \frac{\partial g_1^i}{\partial y_1}, \frac{\partial g_4^i}{\partial y_4} + 2\frac{\partial g_5^i}{\partial y_5}, \frac{\partial g_5^r}{\partial x_5} - \frac{\partial g_5^i}{\partial x_6}$	1,1,1,1
	$0, \frac{\partial g_2^r}{\partial x_2}, \frac{\partial g_2^i}{\partial y_2}$	2,2,2
	$\lambda_1^{(5)}, \lambda_2^{(5)}; \lambda_1^{(5)} + \lambda_2^{(5)} = \text{tr } A, \lambda_1^{(5)}\lambda_2^{(5)} = \det A, A = \begin{pmatrix} \frac{\partial g_1^r}{\partial x_1} & 2\frac{\partial g_4^r}{\partial x_5} \\ \frac{\partial g_5^r}{\partial x_4} & \frac{\partial g_5^r}{\partial x_5} + \frac{\partial g_5^i}{\partial x_6} \end{pmatrix}$	1,1
6	$0, \frac{\partial g_4^i}{\partial y_4} - \frac{\partial g_4^i}{\partial y_5} + \frac{\partial g_1^i}{\partial y_1} - \frac{\partial g_1^i}{\partial y_2}$	2,2
	$\lambda_1^{(6)}, \lambda_2^{(6)}; \lambda_1^{(6)} + \lambda_2^{(6)} = \text{tr } A, \lambda_1^{(6)}\lambda_2^{(6)} = \det A, A = \begin{pmatrix} \frac{\partial g_1^r}{\partial x_1} + 2\frac{\partial g_1^r}{\partial x_2} & \frac{\partial g_1^r}{\partial x_4} + 2\frac{\partial g_1^r}{\partial x_4} \\ \frac{\partial g_4^r}{\partial x_1} + 2\frac{\partial g_4^r}{\partial x_2} & \frac{\partial g_4^r}{\partial x_4} + 2\frac{\partial g_4^r}{\partial x_5} \end{pmatrix}$	1,1
	$\lambda_1^{\prime(6)}, \lambda_2^{\prime(6)}; \lambda_1^{\prime(6)} + \lambda_2^{\prime(6)} = \text{tr } B, \lambda_1^{\prime(6)}\lambda_2^{\prime(6)} = \det B, B = \begin{pmatrix} \frac{\partial g_1^i}{\partial y_1} + 2\frac{\partial g_1^i}{\partial y_2} & \frac{\partial g_1^i}{\partial y_4} + 2\frac{\partial g_1^i}{\partial y_4} \\ \frac{\partial g_4^i}{\partial y_1} + 2\frac{\partial g_4^i}{\partial y_2} & \frac{\partial g_4^i}{\partial y_4} + 2\frac{\partial g_4^i}{\partial y_5} \end{pmatrix}$	1,1
	$\lambda_1^{\prime\prime(6)}, \lambda_2^{\prime\prime(6)}; \lambda_1^{\prime\prime(6)} + \lambda_2^{\prime\prime(6)} = \text{tr } C, \lambda_1^{\prime\prime(6)}\lambda_2^{\prime\prime(6)} = \det C, C = \begin{pmatrix} \frac{\partial g_1^r}{\partial x_1} - \frac{\partial g_1^r}{\partial x_2} & \frac{\partial g_1^r}{\partial x_4} - \frac{\partial g_1^r}{\partial x_4} \\ \frac{\partial g_4^r}{\partial x_1} - \frac{\partial g_4^r}{\partial x_2} & \frac{\partial g_4^r}{\partial x_4} - \frac{\partial g_4^r}{\partial x_5} \end{pmatrix}$	2,2
7	$0, \frac{\partial g_4^r}{\partial x_4} - \frac{\partial g_4^r}{\partial x_5} + \frac{\partial g_4^i}{\partial y_4} - \frac{\partial g_4^i}{\partial y_5}$	2,2
	$\lambda_1^{(7)}, \lambda_2^{(7)}; \lambda_1^{(7)} + \lambda_2^{(7)} = \text{tr } A, \lambda_1^{(7)}\lambda_2^{(7)} = \det A, A = \begin{pmatrix} \frac{\partial g_1^r}{\partial x_1} & \frac{\partial g_1^r}{\partial y_1} \\ \frac{\partial g_1^i}{\partial x_1} & \frac{\partial g_1^i}{\partial y_1} \end{pmatrix}$	3,3
	$\lambda_1^{\prime(7)}, \lambda_2^{\prime(7)}; \lambda_1^{\prime(7)} + \lambda_2^{\prime(7)} = \text{tr } B, \lambda_1^{\prime(7)}\lambda_2^{\prime(7)} = \det B, B = \begin{pmatrix} \frac{\partial g_4^r}{\partial x_4} + 2\frac{\partial g_4^r}{\partial x_5} & \frac{\partial g_4^r}{\partial y_4} + 2\frac{\partial g_4^r}{\partial y_5} \\ \frac{\partial g_4^i}{\partial x_4} + 2\frac{\partial g_4^i}{\partial x_5} & \frac{\partial g_4^i}{\partial y_4} + 2\frac{\partial g_4^i}{\partial y_5} \end{pmatrix}$	1,1

Table 4. Eigenvalues, signs of the eigenvalues at the cubic order approximation, and eigenvectors of the Jacobian matrices for the primary solutions.

Label	Eigenvalues	Signs of Eigenvalues	Eigenvectors
2	0		$(0,0,0,0,0,0,0,0,0,1,0,0)^T$
	$\frac{\partial g_1^r}{\partial x_1}$	$\text{sgn}[\sigma_1 - \sigma_2 \mu_{11}/\mu_{21} + \beta_1 x]$	$(1,0,0,0,0,0,0,0,0,0,0,0)^T$
	$\frac{\partial g_1^i}{\partial y_1}$	$\text{sgn}[\sigma_1 - \sigma_2 \mu_{11}/\mu_{21} - \beta_1 x]$	$(0,0,0,0,0,0,0,1,0,0,0,0)^T$
	$\frac{\partial g_4^r}{\partial x_4}$	$\text{sgn}[\mu_{21}]$	$(0,0,0,1,0,0,0,0,0,0,0,0)^T$
	$\frac{\partial g_5^r}{\partial x_5} + \frac{\partial g_6^r}{\partial x_6}$	$\text{sgn}[\sigma_2 - \sigma_2 \mu_{22}/\mu_{21} + \delta_2 x]$	$(0,0,0,0,1,1,0,0,0,0,0,0)^T, (0,0,0,0,0,0,0,0,0,0,1,-1)^T$
	$\frac{\partial g_5^r}{\partial x_5} - \frac{\partial g_6^r}{\partial x_6}$	$\text{sgn}[\sigma_2 - \sigma_2 \mu_{22}/\mu_{21} - \delta_2 x]$	$(0,0,0,0,1,-1,0,0,0,0,0,0)^T, (0,0,0,0,0,0,0,0,0,0,1,1)^T$
	$\frac{\partial g_2^r}{\partial x_2}$	$\text{sgn}[\sigma_1 - \sigma_2 \mu_{12}/\mu_{21}]$	$(0,1,0,0,0,0,0,0,0,0,0,0)^T, (0,0,1,0,0,0,0,0,0,0,0,0)^T, (0,0,0,0,0,0,0,0,1,0,0,0)^T, (0,0,0,0,0,0,0,0,0,1,0,0)^T$
	3	$\frac{\partial g_4^r}{\partial x_4} + 2\frac{\partial g_5^r}{\partial x_5}$	$\text{sgn}[-(2\sigma_2 + \delta_2 x)]$
$3\frac{\partial g_4^i}{\partial y_4}$		$\text{sgn}[-\delta_2 x]$	$(0,0,0,0,0,0,0,0,0,1,1,1)^T$
0			$(0,0,0,0,0,0,0,0,0,1,-1,0)^T, (0,0,0,0,0,0,0,0,0,0,-1,1)^T$
$\frac{\partial g_4^r}{\partial x_4} - \frac{\partial g_5^r}{\partial x_5}$		$\text{sgn}[\sigma_2 + (2\mu_{21} + \mu_{22})x^2]$	$(0,0,0,-1,0,1,0,0,0,0,0,0)^T, (0,0,0,-1,1,0,0,0,0,0,0,0)^T$
$\frac{\partial g_1^r}{\partial x_1}$		$\text{sgn}[\sigma_1 + \beta_1 x + (\mu_{11} + 2\mu_{12} + \nu_1)x^2]$	$(1,0,0,0,0,0,0,0,0,0,0,0)^T, (0,1,0,0,0,0,0,0,0,0,0,0)^T, (0,0,1,0,0,0,0,0,0,0,0,0)^T$
$\frac{\partial g_1^i}{\partial y_1}$		$\text{sgn}[\sigma_1 - \beta_1 x + (\mu_{11} + 2\mu_{12} - \nu_1)x^2]$	$(0,0,0,0,0,0,1,0,0,0,0,0)^T, (0,0,0,0,0,0,0,1,0,0,0,0)^T, (0,0,0,0,0,0,0,0,1,0,0,0)^T$

Table 5. Coefficients of (16) for $P_1 = P_2 = 7$, $G = D^4 R_2/R_1$, and $D = 2.0977$. The critical wavenumbers for all the cases may be well approximated by 2.915.

	ϵ_1/ϵ_2	0.0/0.0	0.1/0.1	0.2/0.2	0.3/0.3	0.4/0.4	0.5/0.5
R_2/R_1		1.0607	1.2180	1.3914	1.5835	1.7973	2.0368
R_1		1401.8	1279.5	1176.6	1088.7	1012.8	946.6
β_1		0.50946	0.53540	0.55531	0.58181	0.60477	0.63582
δ_1		0.0	1.9082	3.4347	4.7715	6.0458	7.1835
κ_{11}		-325.50	-321.93	-316.60	-312.64	-305.09	-303.55
κ_{12}		-456.28	-454.81	-449.96	-445.48	-436.82	-433.41
μ_{11}		0.36106	0.25892	0.18239	0.12669	0.078423	0.043310
μ_{12}		-0.037628	-0.071596	-0.098955	-0.11534	-0.12961	-0.14012
ν_1		-1.0323	-0.88120	-0.77393	-0.69090	-0.62795	-0.57056
ξ_1		0.65685	1.4755	2.2238	2.8963	3.6405	4.3342
η_1		5.2134	3.8575	2.9835	2.3632	2.0204	1.7320
β_2		-45.994	-44.728	-43.581	-42.351	-41.315	-40.006
δ_2		0.0	0.073079	0.13487	0.18834	0.23816	0.27820
κ_{21}		25.755	22.779	20.027	17.180	14.987	12.636
κ_{22}		56.318	52.918	50.167	47.372	44.955	42.596
μ_{21}		-0.56231	-0.43583	-0.34656	-0.27948	-0.22371	-0.18640
μ_{22}		-0.69764	-0.53816	-0.42567	-0.34125	-0.27150	-0.22446
ν_2		-761.24	-717.87	-683.52	-645.30	-610.08	-570.57
ξ_2		11.075	11.255	11.271	11.486	11.609	11.645

ble 6. Coefficients of (16) for $P_2 = 7$, $G = 1$, $D = 2.0977$, and $P_1 = R_2/R_1 \times D^4$
 The critical wavenumbers for all the cases may be well approximated by 2.915.

ϵ_1/ϵ_2	0.0/0.0	0.0/0.1	0.0/0.2	0.0/0.3	0.0/0.4	0.0/0.5
R_2/R_1	1.0607	1.11234	1.1692	1.2321	1.3021	1.3804
R_1	1401.8	1400.8	1399.7	1398.6	1397.2	1395.8
β_1	-1.5978	-1.5598	-1.5164	-1.4661	-1.4064	-1.3370
δ_1	0.0	0.31158	0.64348	1.0199	1.4455	1.9311
κ_{11}	-319.66	-315.87	-311.79	-307.36	-302.54	-297.27
κ_{12}	-771.86	-791.31	-809.36	-824.62	-838.78	-844.40
μ_{11}	-26.736	-29.365	-32.340	-35.707	-39.531	-43.929
μ_{12}	-143.74	-160.03	-178.36	-199.44	-223.55	-251.95
ν_1	-211.99	-237.02	-265.09	-297.54	-334.76	-379.45
ξ_1	-192.77	-205.77	-217.74	-229.10	-239.03	-246.97
η_1	-507.01	-566.82	-631.31	-703.72	-784.94	-879.81
β_2	152.01	166.49	182.28	199.63	218.81	240.17
δ_2	0.0	1.6948	3.5814	5.6928	8.0661	10.767
κ_{21}	351.80	502.46	678.13	884.41	1129.0	1420.8
κ_{22}	7284.3	8763.7	10562	12787	15553	19058.
μ_{21}	-252.58	-261.98	-272.64	-284.59	-297.86	-312.95
μ_{22}	-309.28	-319.17	-330.24	-342.38	-355.55	-370.12
ν_2	47825	58205	70887	86592	106410	131410
ξ_2	5738.9	6953.5	8454.0	10329	12698	15705

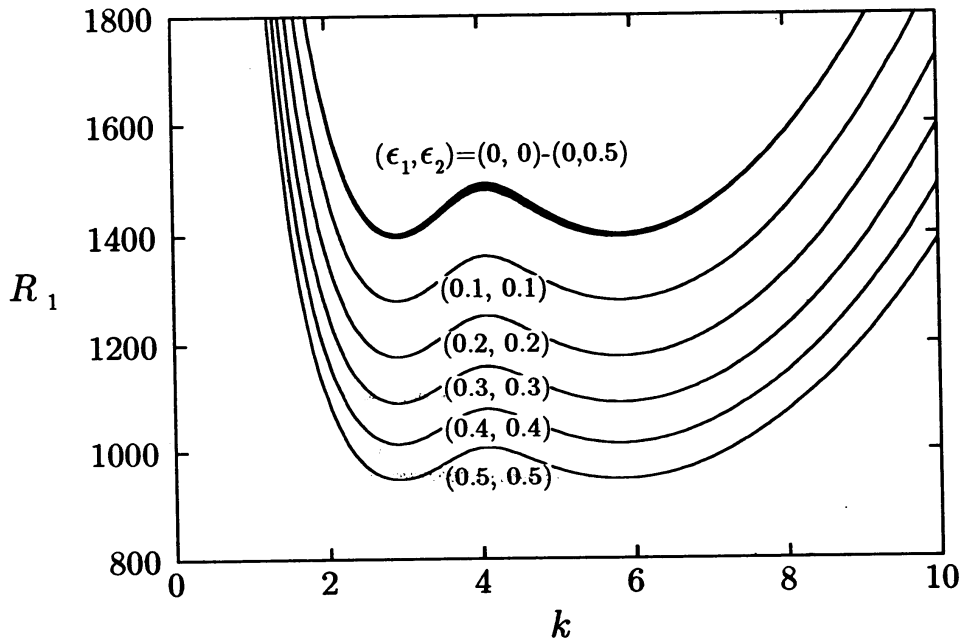


Fig.1. Linear neutral stability curves. $D = 2.0977$.

Table 7. Stability of type 2-6 solution branches.
 $P_1 = P_2 = 7, G = D^4 R_2 / R_1,$ and $D = 2.0977.$

Line Segment	Stability	Line Segment	Stability
2a	0 + + - + - +	6a	0 + * * - + - +
2b	0 + - - + - +	6b	0 + * * - + + +
2c	0 + - - + - -	6c	0 - * * - + * *
2d	0 - - - + - -	6d	0 - * * - + = =
3a	- + 0 + + +	6e	0 - * * - - = =
3b	- + 0 + - +	6a'	0 + - + + + + +
3c	- + 0 + - -	6b'	0 + + + + + + + +
3d	+ - 0 - - -	6c'	0 - * * * * * *
3e	+ - 0 - + -	6d'	0 - * * = = * *
3f	+ - 0 - + +	6e'	0 - * * - - - -
4a	0 + + + - + * *	6f'	0 - * * - - - +
4b	0 + + + - - * *	6g'	0 - - + - - - +
4c	0 - + + - - * *	6f	0 - = = - + - +
4d	0 - - + - - * *	6g	0 - = = - + - -
4e	0 - - + - - = =	6h	0 + = = - + = =
4f	0 - - - + - = =	6i	0 + = = - + * *
4g	0 - - - + + = =	6j	0 + = = + + * *
4h	0 + - - + + = =	6h'	0 - - + - - - -
4i	0 + + - + + = =	6i'	0 - - - - - - -
		6j'	0 + = = = = = =
		6k'	0 + = = * * = =
		6l'	0 + = = + + * *
		6m'	0 + = = + + - +
		6n'	0 + - + + + - +

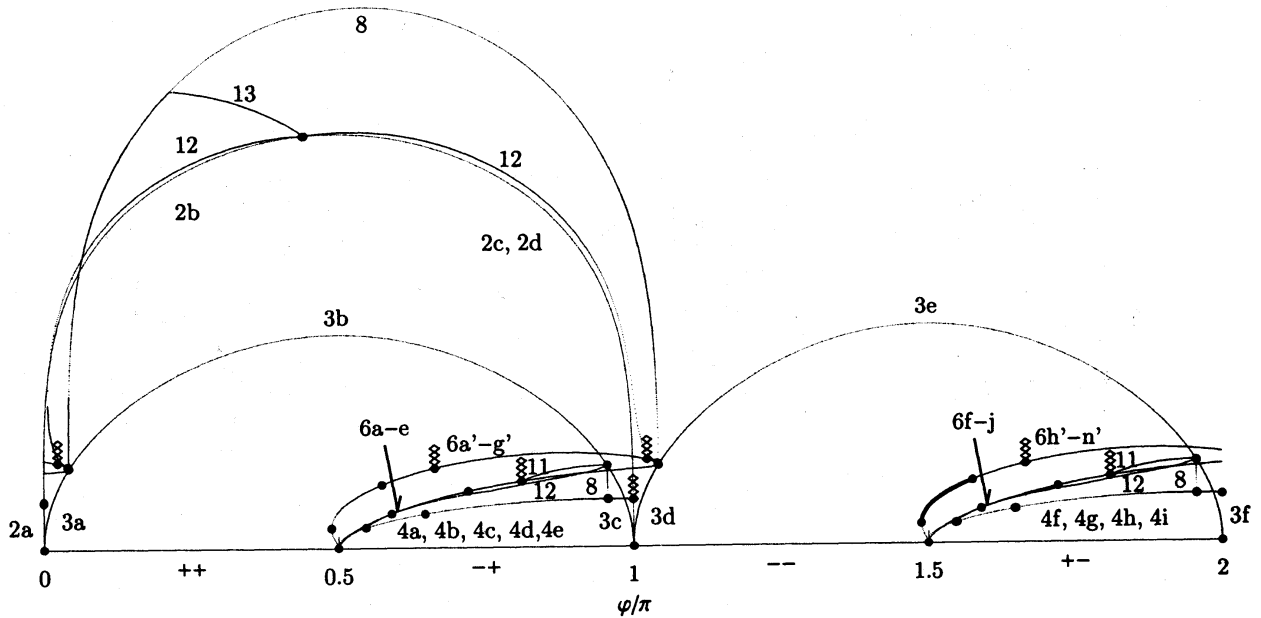


Fig.2. Bifurcation diagram for Table 5, $\epsilon_1 = \epsilon_2 = 0.1.$

Table 8. Stability of type 2-6 solution branches.
 $P_2 = 7, G = 1, D = 2.0977,$ and $P_1 = R_2/R_1 \times D^4 \times P_2.$

Line Segment	Stability	Line Segment	Stability
2a	0 + + - + - +	6a	0 + + + - + + +
2b	0 - + - + - +	6b	0 - + + - + + +
2c	0 - + - + - -	6c	0 - = = - + + +
2d	0 - - - + - -	6a'	0 + + + + + + +
3a	- + 0 + + +	6b'	0 + + + - + + +
3b	- + 0 + + -	6c'	0 - + + - + + +
3c	- + 0 + - -	6d'	0 - = = - + + +
3d	+ - 0 - - -	6d	0 - = = - + - -
3e	+ - 0 - - +	6e	0 + = = - + - -
3f	+ - 0 - + +	6f	0 + + + - + - -
4a	0 + + + - - * *	6e'	0 - - - - - - -
4b	0 - + + - - * *	6f'	0 - - - - + - -
4c	0 - + - - - * *	6g'	0 + = = - + - -
4d	0 - + - - - = =	6h'	0 + + + - + - -
4e	0 - - - + + = =		
4f	0 + - - + + = =		
4g	0 + - + + + = =		

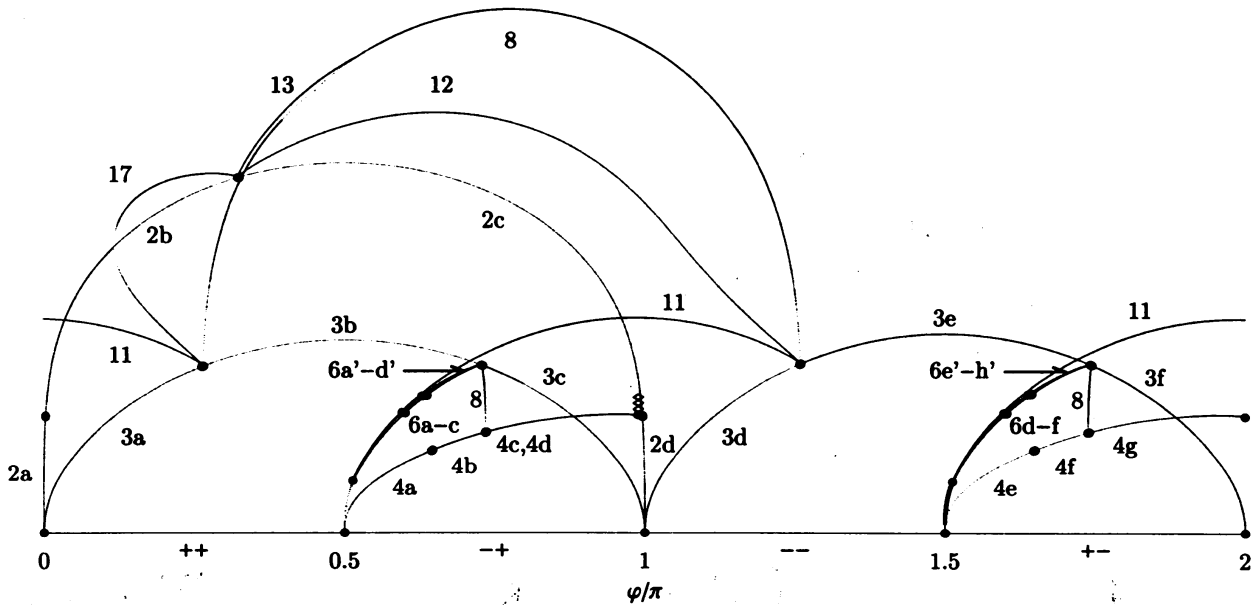


Fig.3. Bifurcation diagram for Table 6, $\epsilon_1 = 0, \epsilon_2 = 0.1.$